AIP Advances

Proton irradiation effects on the thermoelectric properties in single-crystalline Bi nanowires

Taehoo Chang, Jeongmin Kim, Min-Jung Song, and Wooyoung Lee

Citation: AIP Advances **5**, 057101 (2015); doi: 10.1063/1.4919786
View online: http://dx.doi.org/10.1063/1.4919786
View Table of Contents: http://scitation.aip.org/content/aip/journal/adva/5/5?ver=pdfcov
Published by the AIP Publishing

Proton irradiation effects on the thermoelectric properties in single-crystalline Bi nanowires

Taehoo Chang,[a] Jeongmin Kim,[a] Min-Jung Song, and Wooyoung Lee[b]
Department of Materials Science and Engineering Yonsei University, 134 Shinchon, Seoul 120-749, Korea

(Received 15 February 2015; accepted 21 April 2015; published online 1 May 2015)

The effects of proton irradiation on the thermoelectric properties of Bi nanowires (Bi-NWs) were investigated. Single crystalline Bi-NWs were grown by the on-film formation of nanowires method. The devices based on individual Bi-NWs were irradiated with protons at different energies. The total number of displaced atoms was estimated using the Kinchin-Pease displacement model. The electric conductivity and Seebeck coefficient in the Bi-NW devices were investigated before and after proton irradiation at different temperatures. Although the Seebeck coefficient remained stable at various irradiation energies, the electrical conductivity significantly declined with increasing proton energy up to 40 MeV. [http://dx.doi.org/10.1063/1.4919786]

I. INTRODUCTION

Thermoelectric devices have attracted great research interest as they can directly convert thermal energy to electricity, and vice versa, through Seebeck and Peltier effects.[1–5] Although the applicability of the thermoelectric effect to power generators and coolers is restricted by the limited efficiency of energy conversion,[4–6] it is still important for power generation systems (e.g., radioisotope thermoelectric generators, RTG) in extreme environments (such as long-term space exploration).[7–10] The thermoelectric efficiency is determined by the figure of merit (ZT), defined as $ZT = S^2\sigma T/\kappa$.[11] Here, S, σ, κ, and T are the Seebeck coefficient, electrical conductivity, thermal conductivity, and temperature, respectively. For a high ZT value, the Seebeck coefficient and electric conductivity must be large, while the thermal conductivity must be small. These parameters are influenced by the composition and structure of the thermoelectric materials.[4,6,12–14] Particularly, the solar energy particle events, occurring with the solar flares, consist mainly of protons (90%) which were not only over 100 MeV usually but also up to 1GeV.[15] Moreover, Proton irradiation causes structural damage in semiconductor devices, such as ionization and displacement.[16–19] Ionization damage leads to changes of the surface state at the interface between the semiconductor crystal and the insulating layer.[19–21] Concurrently, the displacement damage creates additional defects in the semiconductor crystal as well as degradation of the device characteristics.[22] Similarly to semiconductor devices, thermoelectric materials are exposed to radiation damages in space. Therefore, it is necessary to investigate the radiation effects on semiconductor devices in relation to their application in severe radiation environments such as space, accelerators, and nuclear facilities. In a previous report, we found that the thermal conductivity of single-crystalline Bi nanowires (Bi-NWs) approximately decreases by half after proton irradiation.[23] The Bi-NWs have been regarded as promising thermoelectric materials because of the enhancement of ZT due to the quantum confinement effect.[4,24,25] Such an effect, predicted by theoretical studies, originates from a very small effective mass, large Fermi wavelength, and small band overlap of semimetal Bi. According to

[a]T. Chang and J. Kim contributed equally to this work.
[b]Author to whom correspondence should be addressed. Electronic mail: wooyoung@yonsei.ac.kr

the relation between ZT and κ, a reduction of thermal conductivity due to the proton irradiation causes an increase in ZT. However, to estimate the correct variation of ZT by proton irradiation, the quantitative change of electrical thermoelectric properties (σ and S) should also be considered. In this study, we investigated the variation of the thermoelectric properties as a function of the proton energy at various temperatures. The proton irradiation effect on the thermoelectric figure of merit was estimated by comparing the change of σ and S with that of κ reported in the previous study.

II. EXPERIMENTALS

A. Preparation of the Bi-NW device

To fabricate devices based on an individual NW, single-crystalline Bi-NWs were grown by the on-film formation of nanowires (OFFON) method. The details of the growth mechanism and device preparation are available elsewhere.[26] Briefly, a 50 nm-thick Bi film was deposited onto a Si/SiO_2 substrate using RF sputtering and then annealed in a furnace at 250 °C for 5 h under ultra-high vacuum. The as-grown Bi-NWs were dispersed on a thermally oxidized Si/SiO_2 (500 nm SiO_2) substrate with the align markers patterned by photolithography. Au electrodes and a microheater were fabricated using e-beam lithography and a lift-off process. Before deposition of Cr/Au (5 nm/250 nm) electrodes, the Bi-NW was treated using Ar plasma to remove any native oxide on their surface; this process was performed under vacuum to prevent additional oxidation. The deposition was carried out using a DC magnetron sputtering system (custom-made) at a base pressure of 4×10^{-7} Torr. Although ZT of Bi NWs was expected to increase as decreasing diameter in the previous theoretical studies,[4,24,25] the experimental investigation using the [100] oriented Bi NWs grown by OFFON method demonstrated the optimization of ZT at the diameter range of 100–150 nm.[27] Therefore, four Bi-NW devices with diameters of 116 nm (NW1), 118 nm (NW3), 148 nm (NW2), and 165 nm (NW4) were prepared for the measurement of thermoelectric properties.

B. Measurement and characterization

Figure 1(a) shows a Bi-NW device observed with a field-emission scanning electron microscope (FE-SEM; JSM-7001F). The Bi-NW device consists of a microheater, two thermometers, and two additional electrodes; a four-point probe technique was used to remove the contact resistance by connecting four electrodes to the Bi-NW.[28,29] The microheater was located at 0.5 μm from one thermometer and the distance between the two thermometers was set at 2 μm. All electrical measurements were performed in a cryostat (custom-made), monitoring the thermal stability. To investigate the effects of proton irradiation, the Bi-NW devices were irradiated in a MC-50 cyclotron system (Korea Institute of Radiological and Medical Sciences) (Figure 1(b)). The samples are summarized in Table I according to their irradiation parameters. The crystallographic structure of the irradiated Bi-NWs was analyzed using high-resolution transmission electron microscopy (HR-TEM; JEM-2100F) with selected area electron diffraction (SAED) pattern. The cross-sectional specimens were prepared by focused ion beam (FIB; NOVA 600 Nanolab).

The thermoelectric properties (σ and S) of all the samples were measured before and after irradiation, repeating the process to evaluate their reliability. To measure the electrical conductivity (σ) of the Bi-NW, the I-V curve was obtained using a four-point probe technique with a data-acquisition system (DAQ 6259, National Instruments) and a nanovoltmeter (2182, Keithley). The electrical conductivity is inversely related to the electrical resistivity (ρ), which is defined as $\rho = R \times A/l$ where R, l, and A are the resistance, channel length, and the cross-sectional area of the Bi-NW. The resistance was obtained by linear fitting of the measured I-V curve. For the measurement of the Seebeck coefficient (S), a temperature gradient along the Bi-NW was generated by Joule heating applying heater voltage to the microheater. The Seebeck voltage (ΔV) between two thermometers was measured by the nanovoltmeter and the resistance of each thermometer was determined by lock-in amplifiers (SR850, Stanford Research Systems) to obtain the temperature difference (ΔT). From the measured data, the Seebeck coefficient was calculated according to the

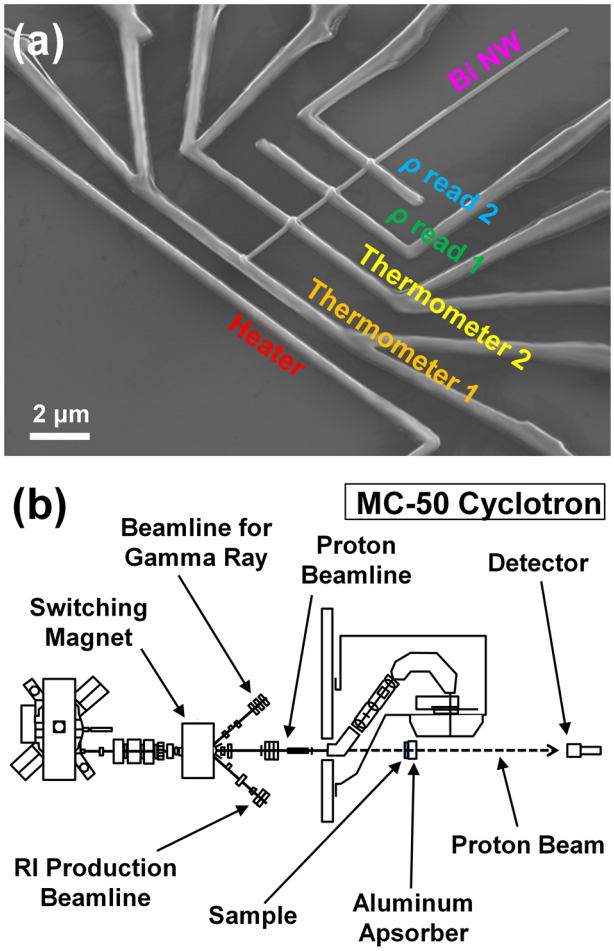

FIG. 1. (a) SEM image of a device based on an individual Bi-NW. (b) Schematic of MC-50 cyclotron for proton irradiation.

relation $S = \Delta V/\Delta T$. It is noted that the measured Seebeck coefficient was corrected by subtracting the portion of the Au thermometers, assuming bulk Au Seebeck coefficient.

III. RESULTS AND DISCUSSION

The HR-TEM images and the corresponding SAED diffraction patterns of the as-grown and irradiated Bi-NWs are shown in Figure 2. The as-grown Bi-NW was a high-quality single crystal with [100] growth direction (Figure 2(a)). The distance of fringes were d = 3.74 Å for $(0\bar{1}1)$ plane and d = 3.96 Å for (003) plane, which nearly correspond to the values of the bulk Bi lattice parameter (a = 4.5460 Å, c = 11.862 Å).[30] The proton-irradiated Bi-NW shows major spots corresponding to the as-grown nanowire, as well as other spots and weak ring shape patterns (Figure 2(b)). This result indicates that proton irradiation partially creates many defects (e.g., point defects and dislocations), resulting in a degradation of the natural crystallinity of the Bi-NW.

TABLE I. Proton irradiation condition of Bi-NW samples.

Sample	Diameter (nm)	Proton E (MeV)	Dose (cm^{-2})
NW1	116	17.2	5×10^{12}
NW2	148	17.2	5×10^{12}
NW3	118	18.9	5×10^{12}
NW4	165	40.0	5×10^{12}

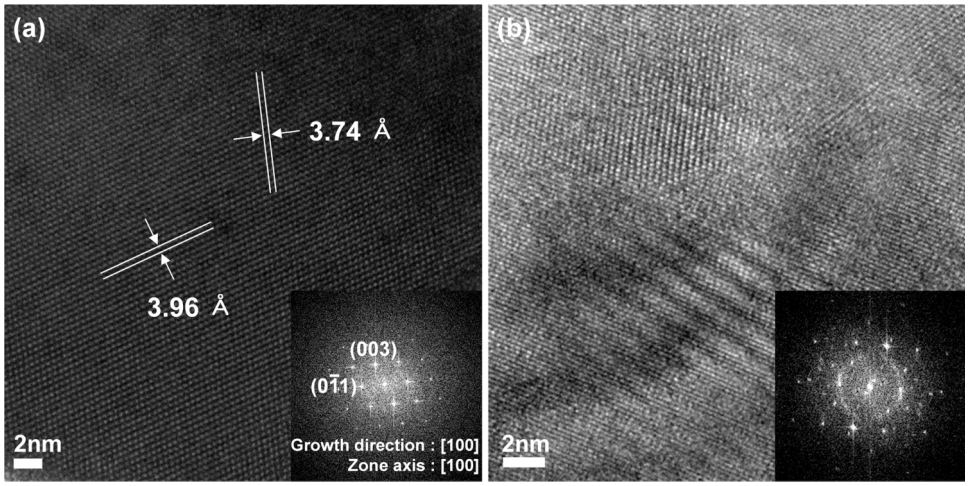

FIG. 2. HR-TEM images of (a) as-grown and (b) proton irradiated Bi-NWs. The samples were prepared by slicing with a FIB the Bi-NWs in a direction normal to the growth direction. The insets show SAED patterns of the NWs obtained by Fourier transformation. The zone axis of the as-grown Bi NW indicated that the OFFON growth direction is [100].

Exposure to high energy radiation generally causes three main processes: (1) production of displaced electrons (i.e., ionization); (2) production of displaced atoms by elastic collision; (3) production of fission and thermal spikes.[31] Among these processes, production of displaced atoms is influenced by the energy received by a lattice atom (E_p).[31,32] If E_p was higher than the displacement threshold energy (E_d) in an elastic collision with a bombarding particle, the atoms would be displaced from its lattice position, producing fundamental displacement pairs (i.e., interstitial and vacancy).[31,32] Thus, more displacement pairs are created as E_p increases. The average number of displaced atoms can be theoretically estimated by the Kinchin-Pease displacement model.[32] The average number of atoms displaced per unit volume (N_d) is given by[32]

$$N_d = \phi t n_0 \sigma_d \bar{v} E_{p\,max}/2E_d, \tag{1}$$

where ϕ, t, n_0, and σ_d are the bombarding flux density, bombardment time, atoms per unit volume, and cross-section per atom, respectively. The maximum energy transferred in a collision is given by $E_{p,max} = 4EMm/(\mathrm{M} + \mathrm{m})^2$, where E, M, and m are the applied energy of the incident particle, mass of the struck atom (Bi), and mass of the incident particle (proton), respectively. Because Bi-NWs with diameters over 100 nm exhibit bulk characteristics,[33] E_d of Bi is approximately equal to 13 eV.[34] In relation to the intensity of the proton energy, the number of displaced atoms (N_d) is 6.18×10^{17} atoms/cm^3, 6.79×10^{17} atoms/cm^3, 1.44×10^{18} atoms/cm^3, at 17.2 MeV, 18.9 MeV, and 40.0 MeV, respectively. Compared with the equilibrium vacancy concentration ($N_v = 3.73 \times 10^{16}$ atoms/cm^3),[35] the N_d values of all the irradiated samples were higher. This result indicates that many point defects or complex defects occur due to the vacancies created through exposure to radiation.

Figure 3 shows the electrical thermoelectric properties (σ and S) of the pre- and post-irradiated Bi-NWs at various temperatures in the range 50–300 K. The electric conductivity of the Bi-NW decreased with decreasing temperature, regardless of the irradiation exposure as shown in Figure 3(a). The carrier concentration of semimetallic Bi is significantly influenced by temperature variation as for semiconducting materials because of its small carrier concentration (2.45×10^{18} cm^{-3} at 300 K).[36] Conversely, the temperature dependence of the mobility was suppressed by the surface scattering resulting from spatial restriction of the NW structure. The proton irradiation caused a decrease of the conductivity as well. Since the reduction of the conductivity was observed in the overall temperature range, this result could be attributed to a decrease of mobility resulting from additional scattering sources generated by proton irradiation. Furthermore, the Seebeck coefficient of all the Bi-NWs also decreased with decreasing temperature (Figure 3(b)). This could be explained by recalling the physical meaning of the Seebeck coefficient, namely the entropy carried

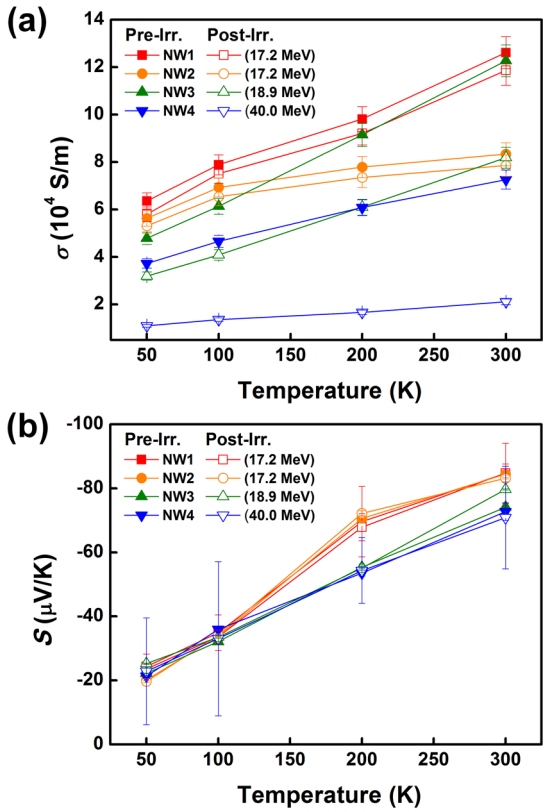

FIG. 3. (a) Electrical conductivity and (b) Seebeck coefficient of Bi-NWs at different temperatures. The solid and open markers represent pre- and post- irradiation data, respectively. The irradiated proton energy varied from 17.2 to 40.0 MeV.

per unit charge in the material, whose value is reduced to zero at the absolute temperature (0 K).[37] Generally, the Seebeck coefficient exhibits the highest values when the Fermi energy locates at the band edge, as it is inversely proportional to the carrier concentration, according to the Mott relation.[6] In the case of Bi, however, the Seebeck coefficient is quite small compared to that of typical semiconductors, because of two different partial bands close to the Fermi energy. In a two band model, the total Seebeck coefficient is determined by the sum of each partial band, with the partial conductivity as weighting factor:[24,38,39]

$$S = \frac{\sigma_e S_e + \sigma_h S_h}{\sigma_e + \sigma_h}, \tag{2}$$

where σ_e, σ_h, S_e, and S_h represent the partial electrical conductivities and the partial Seebeck coefficients of electrons and holes, respectively. Since each partial Seebeck coefficient has opposite sign (negative S_e and positive S_h), the total Seebeck coefficient is very sensitive to the variation of the carrier concentration, contained in the weighting factors. Therefore, the small difference in the Seebeck coefficients before and after irradiation in the overall temperature range suggests that the variation of carrier concentration can be ignored in the process.

Figure 4 shows the electrical thermoelectric properties according to the proton irradiation energy at room temperature. As shown in Figure 4(a), the electrical conductivities of the four samples decreased by about 5.9%, 5.7%, 33.3%, and 70.9% after irradiation exposure for the NW1, NW2, NW3, and NW4, respectively. This result indicates that the electrical conductivity changes more markedly as the proton energy increases. The difference in electrical conductivity of each NWs before irradiation exposure could be attributed to the uncertainty of NW dimension; While the cross-sectional area of NW was estimated form measured diameter, the cross-section deviated from a perfect circle practically. Although this deviation leads to additional error in absolute values of

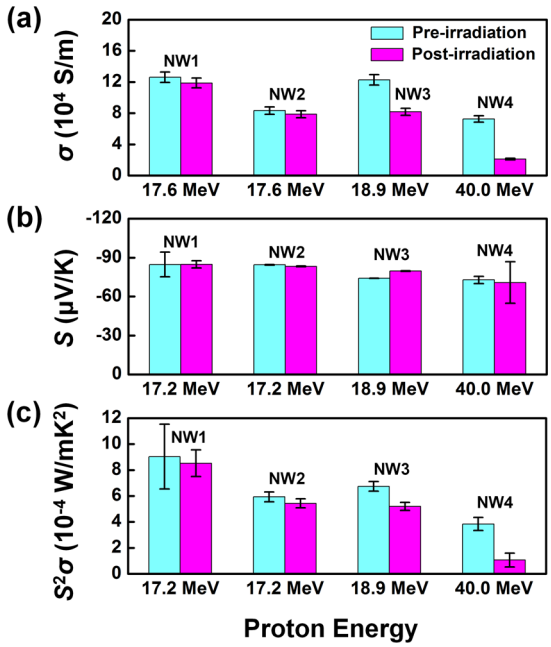

FIG. 4. Histograms of (a) electrical conductivity, (b) Seebeck coefficient, and (c) power factor in Bi-NWs at room temperature. The cyan and magenta bars represent the data of pre- and post-irradiation, respectively.

electrical conductivity, it could be negligible in comparing between before and after proton irradiation because of the unvaried contribution of the deviation. Conversely, Seebeck coefficient of each NWs were very similar because the measured Seebeck voltage didn't include dimension of materials. The relative change of the Seebeck coefficients with the proton irradiation can be ignored in comparison with its error range (Figure 4(b)). The carrier concentration was not affected by the proton irradiation as the Seebeck coefficient of the Bi is very sensitive to the carrier concentration, as mentioned above.[39] The slight increase in the Seebeck coefficient of the NW3 sample might result from the unstable surrounding temperature during the measurement. Consequently, the proton irradiation affects only the carrier mobility by increasing the scattering sources due to damage of the Bi-NW crystallographic structure and leading to a decrease of the electrical conductivity. The power factor (*PF*), which is a charge transport thermoelectric factor, is defined by the electrical conductivity and Seebeck coefficient as $PF = \sigma S^2$. As shown in Figure 4(c), the power factor for the NW1, NW2, NW3, and NW4 samples decreased to 5.6%, 8.4%, 23.0%, and 72.4%, respectively.

Figure 5 shows the normalized changes of the power factor in Bi-NW, before and after proton irradiation, with the proton energy. Although the Seebeck coefficient was found to remain in

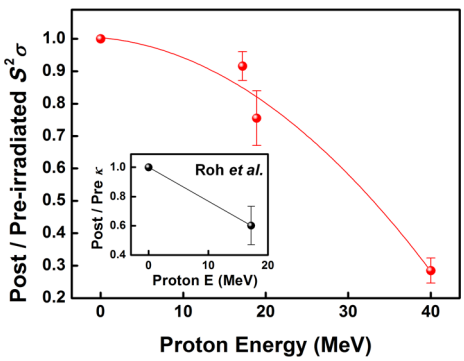

FIG. 5. The variation of power factor in Bi-NW as function of the proton energy. The post-irradiated values were normalized by the pre-irradiated values, and a normalized value at a specific proton energy included all measured data obtained at that proton energy. The inset shows the variation of normalized thermal conductivity which was taken from reference 23.

the measured range, the post-irradiation power factor decreased as the proton energy increased, following a non-linear relation whose rate of reduction rose with the proton energy. For irradiation exposures with energy of 40 MeV, the power factor was reduced by more than 70%. This could be attributed to the reduction of the mean free path due to scattering. Inset shows the normalized changes of the thermal conductivity which were taken from Ref. 23 in order to compare the change of the thermoelectric properties (σS^2 and κ). In general, the thermal conductivity cannot decrease by disorder below a certain value, known as the amorphous limit of κ.[12] The total thermal conductivity consists of two factors: electron thermal conductivity (κ_e) and lattice vibration (phonon) thermal conductivity (κ_{ph}). Heat is transported by phonon at an amorphous state where the crystallization is completely destroyed.[12] If the carrier concentration or mobility was extremely small, the κ_e might be neglected. Although there was significant change of the power factor with proton energy smaller than 40 MeV, ZT cannot decline at irradiation energies below 17.6 MeV because of a reduction of power factor smaller than that of the thermal conductivity at 17.6 MeV. However, the reduction of power factor was more pronounced at higher irradiation energy than 17.6 MeV. Moreover, the electrical conductivity of the total thermoelectric generator system was influenced by various parameters, such as conductance of thermoelectric material and electrodes, contact resistance, and so on. Thus, high-energy particles like protons may have a large and negative effect on electrical thermoelectric factors.

IV. CONCLUSION

The effects of proton irradiation on the thermoelectric properties of the single-crystalline Bi-NWs grown by the OFFON method were investigated using a specially designed device based on an individual NW. The Bi-NW devices were irradiated at different energies and the change of electrical conductivity and Seebeck coefficient due to proton irradiation was measured at several temperatures. All the Bi-NWs exhibited a decrease of electric conductivity with increasing proton energy, regardless of the temperature, due to the damage of the crystal structure. Conversely, the Seebeck coefficients remained stable, indicating that the proton irradiation affects the crystal structure and decrease the mobility, but not the carrier concentration. Based on the measured properties, the power factor was found to decrease faster with increasing proton energy. Although both the obtained power factor and thermal conductivity decreased with increasing proton energy, at proton energy of lower than 17.6 MeV, ZT was found to be determined predominantly by the thermal conductivity. Consequently, this study reports crucial results in relation to the application of Bi-NW devices in severe radiation environments, providing valuable knowledge for the development of future thermoelectric devices.

ACKNOWLEDGMENTS

This work was supported by the National Research Foundation of Korea (NRF) grant funded by the Korea government (MSIP) (2014R1A2A1A10053869), and the Priority Research Centers Program (2009-0093823) and the Pioneer Research Center Program (2013008070) through the NRF funded by the Ministry of Education, Science and Technology.

[1] S. B. Riffat and X. Ma, Appl. Therm. Eng. **23**, 913 (2003).
[2] P. Wang, A. Bar-Cohen, B. Yang, G. L. Solbrekken, and A. Shakouri, J. Appl. Phys. **100**, 014501 (2006).
[3] A. Majumdar, Science **303**, 777 (2004).
[4] M. S. Dresselhaus, G. Chen, M. Y. Tang, R. Yang, H. Lee, D. Wang, Z. Ren, J. P. Fleurial, and P. Gogna, Adv. Mater. **19**, 1043 (2007).
[5] A. Boukai, K. Xu, and J. R. Heath, Adv. Mater. **18**, 864 (2006).
[6] G. J. Snyder and E. S. Toberer, Nat. Mater. **7**, 105 (2008).
[7] R. G. Lange and W. P. Carroll, Energy Conv. Manag. **49**, 393 (2008).
[8] G. L. Bennett, in *4th International Energy Conversion Engineering Conference and Exhibit*, *San Diego, California, AIAA*, *2006* (2006), p. 4191.
[9] R. C. O'Brien, R. M. Ambrosi, N. P. Bannister, S. D. Howe, and H. V. Atkinson, J. Nucl. Mater. **377**, 506 (2008).
[10] H. R. Williams, R. M. Ambrosi, N. P. Bannister, P. Samara-Ratna, and J. Sykes, Int. J. Energy Res. **36**, 1192 (2012).
[11] J. P. Heremans, M. S. Dresselhaus, L. E. Bell, and D. T. Morelli, Nat. Nanotechnol. **8**, 471 (2013).

[12] A. I. Hochbaum, R. Chen, R. D. Delgado, W. Liang, E. C. Garnett, M. Najarian, A. Majumdar, and P. Yang, Nature **451**, 163 (2008).
[13] Y. Lin, X. Sun, and M. S. Dresselhaus, Phys. Rev. B **62**, 4610 (2000).
[14] K. Biswas, J. He, Q. Zhang, G. Wang, C. Uher, V. P. Dravid, and M. G. Kanatzidis, Nat. Chem. **3**, 160 (2011).
[15] E. Verrelli and D. Tsoukals, in *Radiation Hardness of Flash and Nanoparticle Memories*, edited by I. Stievano (InTech, Rijeka, 2011), Vol. 11.
[16] G. R. Hopkinson, C. J. Dale, and P. W. Marshall, IEEE Trans. Nucl. Sci. **43**, 614 (1996).
[17] E. Miyata, H. Kouno, D. Kamiyama, T. Kamazuka, M. Mihara, M. Fukuda, K. Matsuta, H. Tsunemi, T. Minamisono, H. Tomida, and K. Miyaguchi, Jpn. J. Appl. Phys. **42**, 4564 (2003).
[18] G. P. Summers and R. J. Walters, IEEE Trans. Nucl. Sci. **40**, 1372 (1993).
[19] J. R. Srour, C. J. Marshall, and P. W. Marshall, IEEE Trans. Nucl. Sci. **50**, 653 (2003).
[20] G. C. Messenger, *Radiation and its Effects on Devices and Systems* (1991), p. 35.
[21] A. L. Barry, A. J. Houdayer, P. F. Hinrichsen, W. G. Letourneau, and J. Vincent, IEEE Trans. Nucl. Sci. **42**, 2104 (1995).
[22] X. Sun, D. Reusser, H. Dautet, and J. B. Abshire, IEEE Trans. Electron Devices **44**, 2160 (1997).
[23] J. W. Roh, D. H. Ko, J. Kang, M. K. Lee, J. H. Lee, C. W. Lee, K. H. Lee, J. S. Noh, and W. Lee, Phys. Status Solidi A **210**, 1438 (2013).
[24] L. D. Hicks and M. S. Dresselhaus, Phys. Rev. B **47**, 12727 (1993).
[25] L. D. Hicks and M. S. Dresselhaus, Phys. Rev. B **47**, 16631 (1993).
[26] W. Shim, J. Ham, K. Lee, W. Y. Jeung, M. Johnson, and W. Lee, Nano Lett. **9**, 18 (2009).
[27] J. Kim, S. Lee, Y. M. Brovman, P. Kim, and W. Lee, Nanoscale, doi:10.1039/C4NR06412G (2015).
[28] J. Kim, S. Lee, Y. M. Brovman, M. Kim, P. Kim, and W. Lee, Appl. Phys. Lett. **104**, 043105 (2014).
[29] J. Kim, D. Kim, T. Chang, and W. Lee, Appl. Phys. Lett. **105**, 123107 (2014).
[30] D. Schiferl and C. S. Barrett, J. Appl. Crystallogr. **2**, 30 (1969).
[31] A. C. Damask and G. J. Dienes, *Point Defects in Metals*, Professional Edition (Gordon and Breach Science Publisher, New York, 1963), pp. 58–69.
[32] G. H. Kinchin and R. S. Pease, Rep. Prog. Phys. **18**, 1 (1955).
[33] W. Shim, J. Ham, J. Kim, and W. Lee, Appl. Phys. Lett. **95**, 232107 (2009).
[34] P. Bois and F. Beuneu, J. Phys. F : Met. Phys. **17**, 2365 (1987).
[35] N. Matsuno, J. Phys. Soc. Jpn. **42**, 1675 (1977).
[36] Z. Zhang, X. Sun, M. S. Dresselhaus, J. Y. Ying, and J. Heremans, Phys. Rev. B **61**, 4850 (2000).
[37] Y. M. Zuev, W. Chang, and P. Kim, Phys. Rev. Lett. **102**, 096807 (2009).
[38] M. S. Dresselhaus, G. Dresselhaus, X. Sun, Z. Zhang, S. B. Cronin, and T. Koga, Phys. Solid State **41**, 679 (1999).
[39] J. Heremans and C. M. Thrush, Phys. Rev. B **59**, 12579 (1999).